Agricultural and Forest Meteorology 271 (2019) 1–11

Contents lists available at ScienceDirect

Agricultural and Forest Meteorology

journal homepage: www.elsevier.com/locate/agrformet

Inter- and intra-annual dynamics of photosynthesis differ between forest floor vegetation and tree canopy in a subarctic Scots pine stand

Liisa Kulmala[a,b,*], Jukka Pumpanen[c], Pasi Kolari[a,d], Sigrid Dengel[e], Frank Berninger[a], Kajar Köster[a], Laura Matkala[a], Anni Vanhatalo[a], Timo Vesala[a,d], Jaana Bäck[a]

[a] Institute for Atmospheric and Earth System Research / Forest Sciences, Faculty of Agriculture and Forestry, PO Box 27, 00014, University of Helsinki, Helsinki, Finland
[b] Finnish Meteorological Institute, PO Box 503, FI-00101, Helsinki, Finland
[c] Department of Environmental and Biological Sciences, University of Eastern Finland, PO Box 1627, FI-70211, Kuopio, Finland
[d] Institute for Atmospheric and Earth System Research / Physics, Faculty of Science, PO Box 64, 00014, University of Helsinki, Finland
[e] Climate Sciences Department, Lawrence Berkeley National Laboratory, USA

ARTICLE INFO

Keywords:
Eddy covariance
Net ecosystem exchange
Sink limitation

ABSTRACT

We studied the inter- and intra-annual dynamics of the photosynthesis of forest floor vegetation and tree canopy in a subarctic Scots pine stand at the northern timberline in Finland. We tackled the issue using three different approaches: 1) measuring carbon dioxide exchange above and below canopy with the eddy covariance technique, 2) modelling the photosynthesis of the tree canopy based on shoot chamber measurements, and 3) upscaling the forest floor photosynthesis using biomass estimates and available information on the annual cycle of photosynthetic capacity of those species. The studied ecosystem was generally a weak sink of carbon but the sink strength showed notable year-to-year variation. Total ecosystem respiration and photosynthesis indicated a clear temperature limitation for the carbon exchange. However, the increase in photosynthetic production was steeper than the increase in respiration with temperature, indicating that warm temperatures increase the sink strength and do not stimulate the total ecosystem respiration as much in the 4-year window studied. The interannual variation in the photosynthetic production of the forest stand mainly resulted from the forest floor vegetation, whereas the photosynthesis of the tree canopy seemed to be more stable from year to year. Tree canopy photosynthesis increased earlier in the spring, whereas that of the forest floor increased after snowmelt, highlighting that models for photosynthesis in the northern area should also include snow cover in order to accurately estimate the seasonal dynamics of photosynthesis in these forests.

1. Introduction

Northern forests experience cold and snowy winters and a short and cold growing season. Although the carbon uptake rates are smaller than in more southern ecosystems, boreal forests have been traditionally considered to be carbon sinks due to very slow decomposition rates (Fan et al., 1998), but the magnitude of, and the factors that control, this sink are still not accurately quantified. This vulnerable region is predicted to experience extensive climate change, which will influence the carbon exchange between the ecosystem and the atmosphere. Studies have suggested that the photosynthetic uptake, i.e. the primary production of these northern forests, will increase (Myneni et al., 1997; Qian et al., 2010; Ueyama et al., 2015). At the same time, it is known that decomposition is temperature dependent (Davidson and Janssens, 2006) and that increases in plant productivity might increase the soil organic matter decomposition rates (Hartley et al., 2012; Parker et al., 2015). Thus, there is a concern that increased temperature accelerates decomposition and turns these soils from a carbon sink to a source (Crowther et al., 2016).

The typical vegetation structure of northern forests consists of tree canopy and a vegetated and photosynthetically active forest floor. The ground is colonized by a dense community of plant species consisting mainly of ericaceous shrubs, mosses and lichens, whereas relatively sparse canopies above enable notable primary production of the forest floor vegetation (Goulden and Crill, 1997; Moren and Lindroth, 2000; Kulmala, 2011). The proportion of forest floor vegetation in the momentary carbon dioxide (CO_2) uptake of a boreal forest ecosystem has been reported to vary between 3% and 61% (Goulden and Crill, 1997; Subke and Tenhunen, 2004; Ikawa et al., 2015), but the proportion naturally depends on the site, climate and vegetation characteristics.

* Corresponding author.
E-mail address: liisa.kulmala@fmi.fi (L. Kulmala).

https://doi.org/10.1016/j.agrformet.2019.02.029
Received 1 June 2018; Received in revised form 19 February 2019; Accepted 19 February 2019
0168-1923/ © 2019 The Author(s). Published by Elsevier B.V. This is an open access article under the CC BY-NC-ND license (http://creativecommons.org/licenses/BY-NC-ND/4.0/).

Net ecosystem CO_2 exchange is commonly measured by the eddy covariance technique and further partitioned into total ecosystem respiration and photosynthesis, i.e. gross primary production (GPP). The attained total ecosystem photosynthesis consists of the uptake by both the tree canopy and the forest floor vegetation. However, their photosynthetic efficiency and seasonal dynamics differ especially due to their different growth patterns but also due to snow cover that usually continues late into spring, when increased air temperature already enables the photosynthesis of the tree canopy above the snow-covered forest floor. Thus, GPP models which ignore the snow cover might fail to accurately estimate the seasonal dynamics of photosynthesis in northern forests with a sparse tree canopy.

The annual growth is considered to be source limited in many growth models, meaning that the more there is photosynthesis, the more there is growth. However, the growth of northern boreal trees is reported to be temperature, i.e. sink, limited (Körner, 2003), meaning that tree growth in high latitudes is regulated by temperature, which controls the activity of growing meristems, while photosynthetic production together with carbon storage are always sufficient to maintain growth. Several studies have shown that the radial growth, for example, of the northernmost conifers is promoted by warm temperatures during the growing season (Korpela et al., 2011; Seo et al., 2011; Babst et al., 2012; Henttonen et al., 2014; Xu et al., 2014). On the other hand, connections between the growth and GPP have been reported on an annual basis (Berninger et al., 2004; Gea-Izquierdo et al., 2014; Schiestl-Aalto et al., 2015; Kulmala et al., 2016) and on shorter timescales (Chan et al., 2016; Kulmala et al., 2017). However, the research has focused on trees, whereas such studies on sink and source limitation in forest floor vegetation are still missing.

The aim of this study was to explore the intra- and interannual dynamics of forest floor photosynthesis in comparison with those of the tree canopy in a subarctic forest stand. Furthermore, we were interested to see whether the growth of forest floor vegetation is source limited. In addition, we aimed to determine the temperature dependence of the photosynthetic production and ecosystem respiration in order to estimate the effect of rising temperatures on those.

To study these questions, we measured CO_2 fluxes at different scales in a subarctic Scots pine (*Pinus sylvestris* L.) stand at the northern timberline with the eddy covariance technique both above and below the forest canopy and at pine shoot level with shoot chambers. In addition, we measured the variation in the annual height increment of dwarf shrubs on the forest floor. The turbulence needed for eddy covariance measurements is often insufficient below a forest canopy and thus we have also used independent top-down and bottom-up approaches to determine the momentary forest floor photosynthesis. In practice, we downscaled the flux as the difference between the total ecosystem and estimated canopy photosynthesis (top-down), and we upscaled it using the forest floor biomass and available models for leaf-mass based photosynthesis (bottom-up).

2. Materials and methods

2.1. Site

We studied the subarctic Scots pine carbon dynamics over 4 years, between 2012 and 2015, at the Värriö Subarctic Research Station (67° 46′ N, 29° 35′ E), which is located below the northern altitudinal treeline in north-eastern Finnish Lapland. The mean annual temperature was −0.5 °C and the mean annual precipitation 601 mm for the years 1971–2000 (Pirinen et al., 2012). Mean monthly temperature was above 0 °C from May to September. July was the warmest month, with a mean temperature of 13.1 °C.

The study site (SMEAR I) was located on the summit plateau of Kotovaara hill (400 m a.s.l.) and was dominated by Scots pine, with a basal area weighted mean tree height of 10 m and a stem diameter of 14.0 cm. The fell was naturally populated with a density of ~750 trees ha^{-1}. The all-sided leaf area index (LAI) was estimated to be ~3.2 $m^2\,m^{-2}$ using available biomass equations (Repola, 2009), and the specific leaf area was 10 $m^2\,kg^{-1}$. The forest floor vegetation comprised a variety of mosses, lichen and dwarf shrubs such as *Vaccinium myrtillus*, *Vaccinium vitis-idaea* and *Empetrum nigrum*.

2.2. Biomass sampling and the growth of understorey vegetation

The biomass of the forest floor vegetation (vascular plants, mosses and lichen) was estimated by collecting 12 samples in late July 2015 using systematic sampling with a frame (0.198 m × 0.198 m). The samples were divided into different species and weighed separately after drying for 48 h at 60 °C.

Annual height increment of the dwarf shrubs was systematically determined in 2016 using a transect of 45 m length along which we measured the increase in length of the main shoot of the three closest individuals of *V. vitis-idaea*, *V. myrtillus* and *E. nigrum* at 3 m intervals, resulting in 45 individual length increments for each species. The lengths were determined by a digital caliper with an accuracy of 0.01 mm.

All shoot increments were normalized by dividing the increments by the 4-year mean growth of an individual. For example, if a single shoot had grown 15, 20, 10 and 15 mm in the years 2012, 2013, 2014 and 2015, respectively, all increments were divided by their mean, i.e. in this case 15 mm. These relative growths were further statistically analysed. The differences between the years were tested using a one-way analysis of variance (ANOVA) and the Tukey honest significant difference test in R. The difference was considered significant when $p < 0.05$.

2.3. Meteorological measurements

Relative humidity (RH) and ambient air temperature (T_a) at 2 m and 9 m height were measured with MP106 A and PT-100 sensors (Rotronic, Switzerland), respectively, at SMEAR I. The cumulative temperature sum for the growth period was calculated using a 5 °C threshold. Photosynthetically active radiation (PAR) was measured with an LI-190SB Quantum Sensor (LI-COR Biosciences, Lincoln, NE, USA) above the tree canopy. Soil temperature (T_S) was measured 10 cm below ground and in humus (T_H, approx. 2 cm below ground) with a PT-100 sensor. Soil volumetric water content was measured with three ThetaProbe ML2x sensors (Delta-T Devices, UK) located in the uppermost 5 cm. All sensors were located near the eddy covariance tower.

Precipitation (both rain and snowfall) was measured at the Salla Värriötunturi weather station, managed by the Finnish Meteorological Institute and located at the Värriö Subarctic Research Station. Since the forest around SMEAR I is less dense than the area around the research station, the time of snowmelt at SMEAR I was roughly determined from the soil temperature measurements. We assumed that all the snow had melted when the soil temperatures rose above 0.3 °C.

2.4. Eddy covariance instrumentation, data processing and partitioning

The net ecosystem exchange (NEE) of CO_2 was estimated using the eddy covariance (EC) technique, employing the LI-7200 Enclosed Path CO_2/H_2O Analyzer (LI-COR Biosciences) and the METEK USA-1 ultrasonic 3D anemometer (METEK, Elmshorn, Germany) installed at 16.6 m at the top of the eddy flux tower in April 2012.

Net forest floor exchange (NFFE) below the tree canopy was measured at 2.7 m above ground with another eddy covariance system located 25 m away from the main eddy flux tower in 2013. The instrumentation was identical to that above canopy in 2015, but in 2013–2014 an LI-7500 A Open Path CO_2/H_2O Analyzer (LI-COR Biosciences) was used, employing the same model sonic anemometer. The analyser was upgraded to the LI-7200 Enclosed Path CO_2/H_2O Analyzer in spring 2015.

Raw 10 Hz data were processed using standard processing steps with EdiRe (R Clement, University of Edinburgh, UK). The processing included despiking (Vickers and Mahrt, 1997), crosswind correction applicable to the METEK sonic anemometer, coordinate rotation using the two-dimensional rotation method (Baldocchi, 1988), sonic virtual temperature correction (Kaimai and Gaynor, 1991), as well as frequency response correction (Massman, 2000) and buoyancy flux correction (Schotanus et al., 1983). We applied the Webb–Pearman–-Leuning density correction (Webb et al., 1980) to the data originating from the LI-7500 A. We did not apply the Burba correction (Burba et al., 2006, 2008) as the temperature range experienced appeared to be within the limits shown to have no or very little effect on the correction (Burba et al., 2006). Furthermore, the subcanopy system was rarely exposed to direct sunshine for any prolonged amount of time, nor to temperatures below 0 °C. In addition, we applied lag time and tube attenuation corrections relevant to the LI-7200 Enclosed Path CO_2/H_2O Analyzer. In order to guarantee reliable and high-quality flux data, quality checks (Foken and Wichura, 1996; Foken et al., 2004) were carried out. We estimated the footprints (i.e. field of view of the EC setup) of both towers from EC flux data for near-neutral atmospheric stability conditions ($-0.05 < z/L < 0.05$) using the Kormann and Meixner (2001) analytical model. The used thresholds were selected from Geissbühler et al., 2000.

The measured fluxes were corrected for storage change under the measurement height. The storage was calculated from the mean 30-minute CO_2 measurements assuming a constant concentration profile from the measurement height down to the forest floor. Above-canopy fluxes measured under low turbulence were excluded using a friction velocity (u*) threshold of 0.4 m s^{-1} (see later). Below-canopy fluxes were filtered with the standard deviation of vertical wind speed (σ_w) (see Launiainen et al., 2005). The threshold value was 0.2 m s^{-1}. The accepted fluxes were partitioned into GPP (P_E^{EC} or P_{FF}^{EC}) and respiration (R_E or R_{FF}) for the ecosystem (E) and forest floor (FF) using a simple empirical model which was also used for interpolating missing and rejected flux records and analysing the dynamics of CO_2 exchange. The model describes NEE or NFFE as the difference between temperature-driven respiration (R, μmol m^{-2} s^{-1}) and photosynthesis (P, μmol m^{-2} s^{-1}) driven by PAR (I, μmol m^{-2} s^{-1}) and air temperature (T_a, °C). Photosynthesis is modelled as follows:

$$P = \frac{\alpha I + P_{max} - \sqrt{(\alpha I + P_{max})^2 - 4\theta I P_{max}}}{2\theta} f(T) \quad (1)$$

where α, $Pmax$ and θ are parameters. Due to the open canopy and missing forest floor PAR measurements, we used the above-canopy measurements. $f(T)$ is the instantaneous temperature response that brings P to zero at freezing temperatures (Kolari et al., 2014) as follows:

$$f(T) = -\frac{1}{1 + e^{(2(T_0 - T_a))}} \quad (2)$$

where T_0 is the inflection point. Respiration was estimated using an exponential temperature function as follows:

$$R = R_C Q_{10}^{Tsa/10} \quad (3)$$

where R_C and Q_{10} are parameters. The driving temperature T_{sa} was the mean of the air temperature at 9 m height and soil temperature at 10 cm depth. α, $Pmax$ and R_c were estimated for time periods of 11 days, whereas Q_{10} and θ were estimated over the whole study period. The obtained values were $Q_{10} = 2.2$ and $\theta = 0.75$ for the above-canopy data. For the below-canopy data, the obtained values were $Q_{10} = 1.8$ and $\theta = 0.75$.

There was a notable difference in the flux partitioning procedure compared with more southern sites due to the polar day (24 h of daylight): flux records taken in darkness (night-time) were missing in the summer and thus respiration parameters could not be estimated directly from the measured night-time fluxes. Instead, summertime respiration was estimated from the intercept of the regression between NEE and light (see the analysis of this method in Lasslop et al., 2010). Consequently, determining the turbulence filtering criteria (u* and σ_w thresholds) could not be based directly on measured night-time fluxes either. Instead, we performed several model parameterization runs with different u* and σ_w threshold values and determined the final ones as the lowest u* or σ_w thresholds where the estimated R_c was > 98% of the maximum of R_c vs u* or σ_w regression.

When the turbulence criteria were met, P_E^{EC} and P_{FF}^{EC} were calculated as the difference between R_E^{EC} or R_{FF}^{EC} and measured NEE or NFFE, respectively. Missing or rejected NEE (or NFFE) values were gap-filled as the difference between modelled R_E^{EC} (or R_{FF}^{EC}) and P_E^{EC} (or P_{FF}^{EC}).

In order to estimate the uncertainty involved in the gap-filling, we calculated the effect of the used temperature and Q_{10} estimation on the subcanopy fluxes in May–August 2015 using three different Q_{10} values (1.5, 2, 2.5) and two different temperatures (T_{sa} as in Eq. 3 and topsoil temperature at 2 cm depth).

2.5. Carbon dioxide exchange of Scots pine

Gas exchange of Scots pine shoots was automatically measured using four dynamic cylindrical chambers made of acrylic plastic with 3.5 dm^3 volume. The measured shoots were one year old and located at the top of the canopy. The shoots were debudded prior to installation, and thus further shoot elongation inside the chambers was inhibited.

The chambers were open most of the time but one by one they closed for one minute ~180 times a day. CO_2 and water vapour concentrations together with air temperature inside the chambers and PAR outside the chambers were recorded every 10 s during a closure. We calculated the CO_2 exchange rate from the change in the CO_2 concentration in the chamber during a closure. More details on the chamber measurements are available in Hari et al. (1999).

We fitted the optimal stomatal control model (Hari and Mäkelä, 2003; Kolari et al., 2007) to the daily measurements to achieve parameters describing the saturation and initial slope of the light response curve, the temperature response of respiration, and the cost of transpiration. We took a running mean of these parameters over 3 days and used the mean as an input for the Stand Photosynthesis Program (Mäkelä et al., 2006) together with 30-minute averages of measured CO_2 concentration, PAR, air humidity and air temperature to estimate the photosynthesis in the entire canopy, P_C^{SPP}. Instead of upscaling the shoot chamber measurements as such, the model included also tree characteristics and light attenuation in the canopy. Development of a new needle cohort during the summer and shedding of the oldest cohort in the autumn were also described in the model. The leaf area inside the cuvette has little year-to-year variation and thus we normalized the rates of photosynthesis with the ratio between the annual mean of the photosynthetic capacity (β) and the mean β value in 2015. The ratios were 0.73, 0.76, 1.05 and 1 for the years 2012, 2013, 2014 and 2015, respectively.

The downscaled GPP of the forest floor, P_{FF}^{Down}, in 2012–2015 was derived as the difference between P_E^{EC} and P_C^{SPP}:

$$P_{FF}^{Down} = P_E^{EC} - P_C^{SPP}. \quad (4)$$

2.6. Chamber measurements of forest floor carbon dioxide emissions

R_E includes forest floor CO_2 respiration (R_{FF}) and above-ground plant respiration, and thus R_{FF} is expected to be theoretically smaller than R_E. However, several studies have reported lower R_E than R_{FF} at different timescales (Wang et al., 2010; Speckman et al., 2015; Barba et al., 2018). Therefore, we tested the overall level of R_E by measuring R_{FF} twice a month in 2013–2015 in 12 locations using a manual chamber (20 cm in diameter and 25 cm high) and permanently installed collars. These plastic collars (Ø 20 cm) were inserted at a depth of ~3–5 cm into the humus layer around the SMEAR I station in 2012. The chamber was equipped with a small fan and a GMP343 Carbon Dioxide

Table 1
Species-specific parameters for Eqs 5–7 for a 120-year-old Scots pine dominated forest as in Kulmala et al. (2011a). P_0 is the reported maximum P_{max}.

	τ (h)	P_0 (μmol g^{-1} s^{-1})	b (μmol m^{-2} s^{-1})
Vaccinium vitis-idaea	72	0.021	100
Vaccinium myrtillus	150	0.365	107
Calluna vulgaris	120	0.073	200

Probe (Vaisala, Finland) that measured the CO_2 concentration every 5 s. The CO_2 emissions were estimated by a linear ordinary least squares regression of CO_2 concentrations against time during 3.5 min. The CO_2 readings were corrected for temperature and humidity using an HMP75 temperature and humidity probe (Vaisala, Finland). The chamber measurements were performed before noon on rainless days both in ambient light conditions and in darkness when the chamber was enclosed within aluminium foil. The chamber and the flux calculations are described in more detail in Pumpanen et al. (2015).

2.7. Upscaling forest floor vegetation photosynthesis

We modelled species-specific photosynthesis of the vascular forest floor vegetation by estimating leaf-mass based rates of photosynthesis ($\bar{P}$, μmol g^{-1} s^{-1}) for each species based on a simple light response curve (Kulmala et al., 2011a) as follows:

$$\bar{P}(t) = \frac{P_{max}(t)I(t)}{b + I(t)} \quad (5)$$

where $I(t)$ is mean PAR (μmol m^{-2} s^{-1}) above the canopy at hour t and b is a species-specific parameter (Table 1). P_{max} follows changes in the environment and was modelled as follows:

$$P_{max}(t) = f_1(t)f_2(t)f_3(t)P_0 \quad (6)$$

where P_0 is the maximum P_{max} in a 120-year-old forest stand dominated by *P. sylvestris* (Table 1). The function f_1 describes the effect of species-specific temperature history, S, i.e. the state of development (Pelkonen and Hari, 1980; Mäkelä et al., 2004; Kolari et al., 2006). It follows temperature with a species-specific time constant τ (Table 1) as follows:

$$\frac{dS}{dt} = \frac{T(t) - S(t)}{\tau} \quad (7)$$

Kulmala et al. (2011a) used hourly average air temperature as T, but here we decided to use the hourly mean of T_a and T_s since the air temperatures tend to increase earlier than the snow melts. The initial value of S was set to −1 °C, and f_1 was calculated as follows:

$$f_1(t) = \frac{S(t)}{S(t_{st})} \quad (8)$$

Kulmala et al. (2011a) fitted the model based on one measurement on day t_{st}, but here we assume $S(t_{st}) = 15$ °C, i.e. f_1 reaches a maximum with $S(t) = 15$ °C. If S was smaller than 0 °C, f_1 was set to zero.

The function f_2 hinders photosynthesis in low volumetric soil moisture (Φ) conditions as follows:

$$f_2(t) = \begin{cases} 1 & if\ \phi(t) \geq \alpha \\ \phi(t)/\alpha & if\ \phi(t) < \alpha \end{cases} \quad (9)$$

where α is a critical value of volumetric soil moisture after which the soil moisture starts to hinder photosynthesis. We used $\alpha = 0.1$ m^3 m^{-3} as in Kulmala et al. (2011a).

The function f_3 takes into account the carry-over effect from night-time frost (Vesala et al., 2010). It is assigned a value of 1 if the minimum air temperature in the previous 24 h (T_{min}) was above zero. The f_3 value decreases with T_{min} values below 0 °C, reaching zero at −10 °C as follows:

$$f_3(t) = \begin{cases} 1 & if\ T_{min}(t) \geq 0\,°C \\ \frac{T_{min}(t)}{10} + 1 & if\ -10\,°C \leq T_{min}(t) < 0\,°C \\ 0 & if\ T_{min} < -10°C \end{cases} \quad (10)$$

The species-specific $\bar{P}$ values were upscaled to photosynthesis of the forest floor by multiplying the leaf-mass based values by mean leaf biomass, m_i, and summing all species together as follows:

$$P_{FF}^{Up}(t) = \sum_{i=1}^{5} \bar{P}_i(t)m_i. \quad (11)$$

The most abundant vascular plants were *V. vitis-idaea*, *V. myrtillus*, *Vaccinium uliginosum*, *Calluna vulgaris* and *E. nigrum*. Since there were no species-specific parameters available for *V. uliginosum* and *E. nigrum*, we assumed that those were similar to *V. myrtillus* and *C. vulgaris*, respectively. Since our biomass sampling did not separate leaves and stem, we instead used the mean proportion of leaves of the total biomass reported by Kulmala et al. (2011b): 0.62, 0.25 and 0.29 for *V. vitis-idaea*, *V. myrtillus* and *C. vulgaris*, respectively. The proportions of *V. uliginosum* and *E. nigrum* were assumed to be similar to *V. myrtillus* and *C. vulgaris*, respectively. Mosses and lichens are not included in P_{FF}^{Up}.

Using the upscaled rates of forest floor photosynthesis, we derived a second estimate for the photosynthesis of the tree canopy, P_C^{EC-FF}, as follows:

$$P_C^{EC-FF} = P_E^{EC} - P_{FF}^{Up} \quad (12)$$

3. Results

3.1. Weather characteristics

Weather conditions differed greatly during 2012–2015 (Fig. 1ABC, Table 2), allowing interannual comparisons of the ecosystem exchange responses in a wide range of climatic conditions. Growing season 2013 was the warmest, sunniest and driest, with the highest mean temperature and PAR and the lowest precipitation and mean RH. Growing season 2015, on the other hand, was the coldest and moistest, recording the lowest temperature and PAR together with the highest precipitation and mean RH. The other years fell somewhere between these two extremes: 2012 was a cold year and 2014 a warm year, with both recording intermediate mean PAR, RH and precipitation. The winters in 2012 and 2013 were colder than normal, whereas the temperatures in the following winters were typical. The temperature sum ranged from 576 °C in 2015 to 974 °C in 2013.

In all years, daily average temperature occasionally dropped below 5 °C during the growing season. The last night-time frost occurred in late May in all years except 2014, which experienced a cool spell around midsummer, with five nights with freezing temperatures during a period of 10 days.

3.2. Biomass of forest floor vegetation

The most common vascular species of the forest floor vegetation were *V. myrtillus*, *E. nigrum*, *V. vitis-idaea*, *V. uliginosum* and *C. vulgaris*, comprising 27% of the above-ground biomass of forest floor species (Table S1, see Supplementary material). Mosses were the most prevalent group (66%), whereas the proportion of lichens in the total forest floor above-ground biomass was ˜6%.

3.3. Footprint analysis

Fig. 2 illustrates that 80% of the estimated footprint distance (flux contribution) was way below 200 m, especially under favourable conditions along the plateau of Kotovaara hill. The majority or maximum source location (Kljun et al., 2005) of the fluxes originated from the close proximity of the SMEAR I eddy flux tower in the south-western

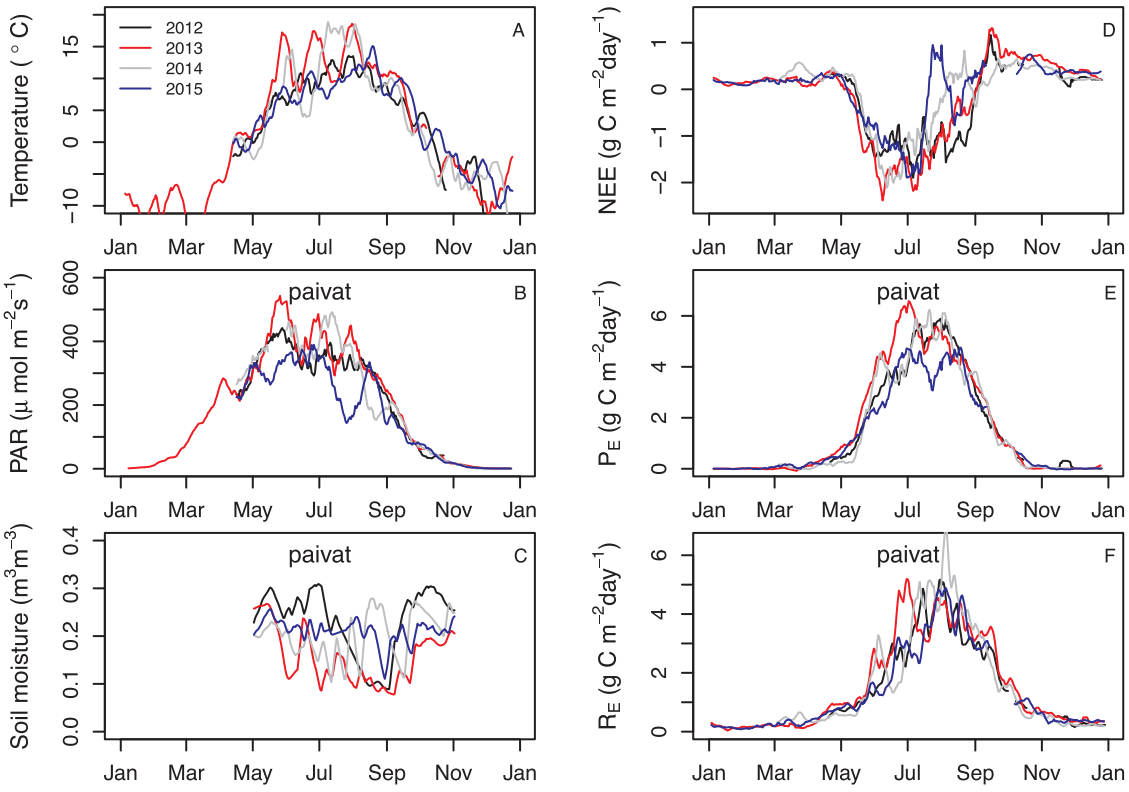

Fig. 1. Daily air temperature (A), daily photosynthetically active radiation (PAR) (B), soil moisture (C), net ecosystem exchange (NEE) (D), gross primary production (P_E) (E) and total ecosystem respiration R_E (F) in 2012–2015. For clarity, the daily rates are moving averages over 10 days except for PAR, which is a moving average over 15 days.

Table 2
Mean meteorological characteristics over the years 2012–2015.

	2012	2013	2014	2015
Mean air temperature Jan–Dec (°C)	−0.6	0.8	0.4	0.5
Mean air temperature May–Sep (°C)	9.2	11.6	10.0	8.5
Temperature sum (°C) [1]	641	974	815	576
Precipitation Jan–Dec (mm)	594	483	601	663
Precipitation Jun–Aug (mm)	192	138	259	252
Beginning of continuous snow cover (yr^{-1})	15 Nov	16 Oct	16 Oct	08 Nov
Greatest snow depth (cm) [2]	87	93	93	82
Date for snowmelt [3]	18 May	16 May	17 May	18 May
Mean PAR [4] May–Aug (µmol m^{-2} s^{-1})	306	341	317	256

[1] With 5 °C threshold. [2] Measured at Värriö Subarctic Research Station. [3] Date when soil temperature rose higher than 0.3 °C. [4] PAR = photosynthetically active radiation.

direction. This distance (roughly 25 m away) corresponds to the location of the subcanopy eddy flux system.

3.4. Ecosystem-scale fluxes

The daily sum of NEE was positive, i.e. the forest was a source of carbon during the off season, transforming into a carbon sink around mid-May (Fig. 1D). Daily NEE returned to positive usually in early September. Daily NEE was sometimes positive during the active season mainly on rainy days accompanied by low radiation. For example, the daily NEE became positive during rainy and cloudy weather in mid-July 2015, when mean daily PAR was only half of the intensity compared with the week before and after (Fig. 1BD). In general, the carbon sink was largest (i.e. NEE was most negative) in June. Due to low turbulence, 34–40% of the 30-minute NEE measurements were missing and were gap-filled during May–September. The missing measurements

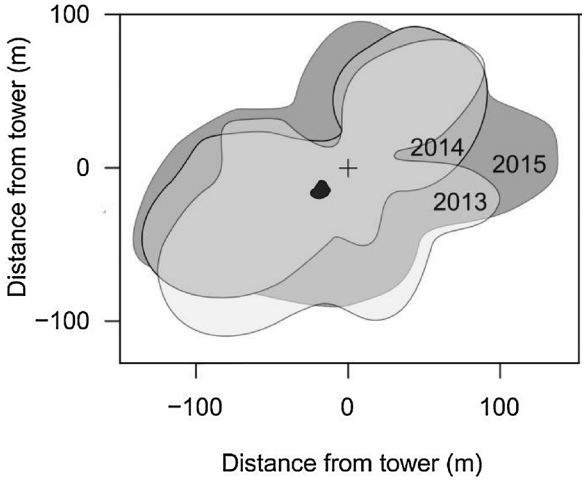

Fig. 2. The different shareds of grey represent the estimated 80% footprint distances around the ecosystem-scale eddy covariance tower (cross) in 2013–2015. For clarity, the small dark area represents the mean 80% footprint distances of the subcanopy eddy covariance system only in 2013 as the other years are comparable with it.

increased the need for gap-filling even more during the snow-covered seasons.

Gap-filled, daily R_E and R_{FF} mostly had a very similar pattern, but R_{FF} was on average 22, 20 and 18% smaller than R_E between 1 May and 31 August in 2013, 2014 and 2015, respectively (Fig. 3). The mean R_{FF} measured with soil chambers was slightly higher or close to R_E (Fig. 3). NFFE suffered from low turbulence close to ground level and technical problems in 2013–2014, resulting in up to 68, 76 and 52% of data being gap-filled during 1 June to 30 September in 2013, 2014 and 2015,

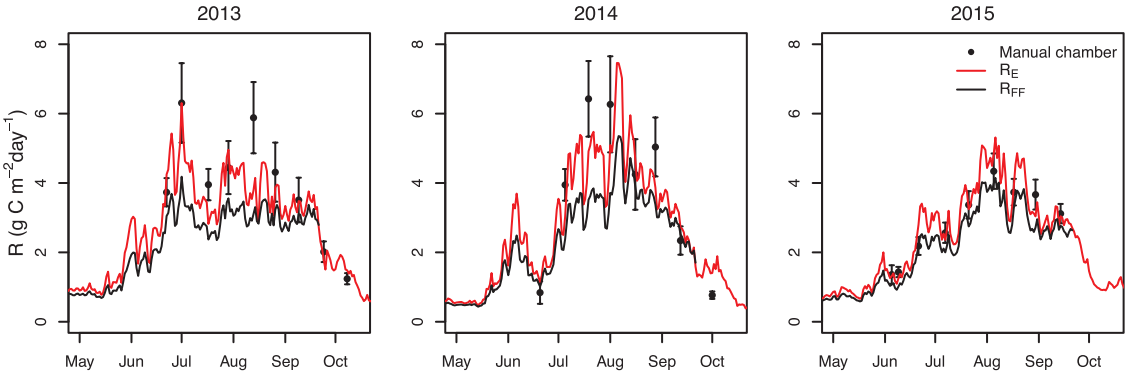

Fig. 3. Mean daily forest floor respiration (R) measured with the manual soil chambers and with eddy covariance above (R_E) and below canopy (R_{FF}) in 2013–2015. The error bars represent the ± standard deviation of the manual chamber measurements (For interpretation of the references to colour in this figure legend, the reader is referred to the web version of this article).

respectively. The range between the minimum and maximum daily NFFE estimates from the different flux partitioning parameterizations was less than 0.43 g C m^{-2} on 90% of the days between 1 May and 30 August. When summing up the whole period, the difference between the minimum and maximum was 5.4 g C m^{-2}, i.e. approx. 5% of the NFFE.

3.5. Forest floor photosynthesis by the three methods

The overall level and annual patterns of the two estimates for forest floor photosynthesis (P_{FF}^{Down} and P_{FF}^{Up}) were comparable especially in the middle of the growing seasons even though in the spring, P_{FF}^{Down} mostly increased later than P_{FF}^{Up} (Fig. 4). P_{FF}^{EC} corresponded to the overall level reached by the other two approaches, but the high need for gap-filling especially in the early and late season made the comparison difficult particularly in 2013 and 2014 (Fig. 5). In 2015, P_{FF}^{Up} followed pretty closely the overall pattern of P_{FF}^{EC}, whereas P_{FF}^{Down} was close to P_{FF}^{EC} in the middle of the season (Fig. 4). The range between the minimum and maximum daily P_{FF}^{EC} estimates by the different flux partitioning parameterizations tested was less than 0.52 g C m^{-2} on 90% of the days between 1 May and 30 August 2015.

3.6. Canopy versus forest floor photosynthesis

Canopy photosynthesis (P_C^{EC-FF}, Eq. 12), already started to increase consistently in all years in April, whereas forest floor photosynthesis, P_{FF}^{Up}, began to increase later, around the time of snowmelt (Fig. 6). The highest daily values of canopy and forest floor photosynthesis were roughly equal in 2013–2014, whereas in 2012 and 2015, the daily rate

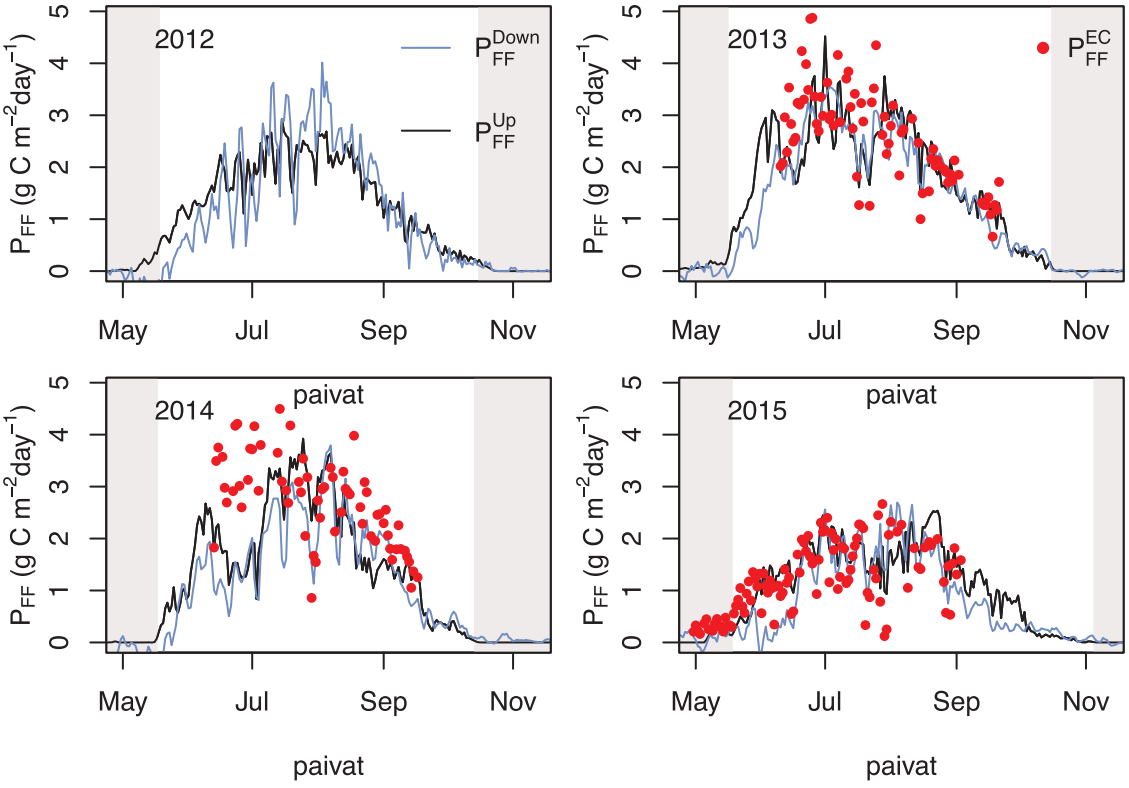

Fig. 4. Daily estimates for forest floor photosynthesis (P_{FF}). P_{FF}^{Down} (Eq. 4) was calculated as the difference between the photosynthesis of the whole ecosystem and the model estimate for canopy photosynthesis. P_{FF}^{Up} was upscaled from mass-based photosynthesis rates (Eq. 11). P_{FF}^{EC} (red dots) are the below-canopy eddy covariance measurements with at least 25% measured daily data. The light grey areas indicate the snow-covered season. For clarity, the series are moving averages over 3 days (For interpretation of the references to colour in this figure legend, the reader is referred to the web version of this article).

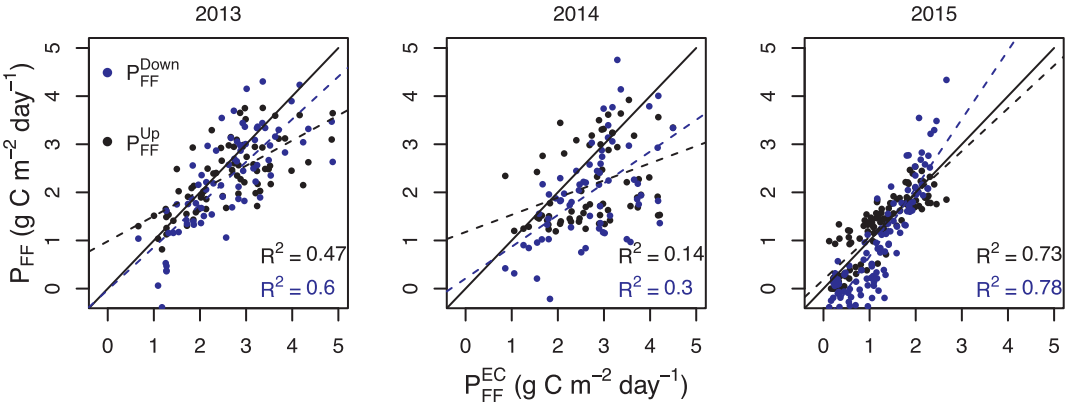

Fig. 5. The two estimates for forest floor photosynthesis (P_{FF}^{Down},blue; P_{FF}^{Up}, black) against below-canopy eddy covariance driven estimate (P_{FF}^{EC}) for those days with at least 25% data coverage of P_{FF}^{EC} measurements. The black line represents a 1:1 linear relationship and the dashed lines represent the linear relationships between measured and modelled data.

of forest floor photosynthesis was mainly lower than that of the canopy. The daily canopy photosynthesis was higher than that of forest floor vegetation on 81, 61, 61 and 68% of days between 1 May and 30 September in 2012, 2013, 2014 and 2015, respectively.

3.7. Annual net ecosystem exchange, respiration and photosynthesis

The stand was a carbon sink (−48 to −7 g C m^{-2} yr^{-1}) during 2012–2014 but a small source of carbon in 2015 (14 g C m^{-2} yr^{-1}, Table 3). The sink was highest in 2013 accompanied by the highest annual P_E^{EC} but also the highest R_E. Both of these were lowest in 2015 (Table 3). The proportion of forest floor photosynthesis relative to the whole ecosystem varied from 43% to 49% when derived using upscaled P_{FF}^{Up} (Eq. 11). It was highest in 2013 (49%) and lowest in 2012 and 2015 (43%).

Annual P_E^{EC} correlated positively with PAR (Table 4, R^2 = 0.92) and temperature sum (R^2 = 0.89), and negatively with precipitation (R^2 = 0.96). Annual R_E correlated positively with temperature sum (R^2 = 0.99) and negatively with precipitation (R^2 = 0.74, not shown). The mean increase in P_E^{EC} with an increase in the temperature sum was 0.27 g C m^{-2} yr^{-1} per degree day, whereas in the case of R_E it was 0.17 g C m^{-2}yr^{-1} per degree day. The different estimates of canopy photosynthesis, P_C^{SPP} and P_C^{EC-FF}, showed very little response to annual variation in temperature sum (0.06–0.08 g C m^{-2} yr^{-1} increase per degree day), whereas the GPP of forest floor vegetation increased more with increasing temperature (0.19–0.21 g C m^{-2} yr^{-1} per degree day)

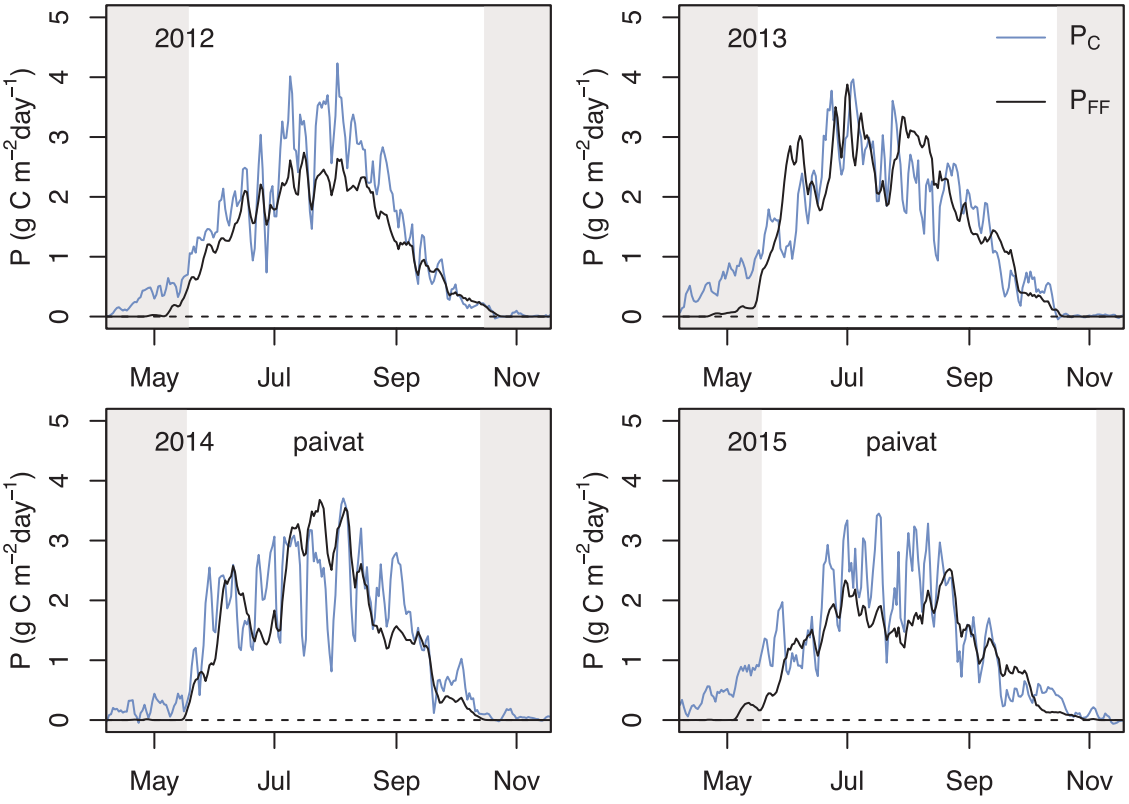

Fig. 6. Daily estimates of the canopy (P_C^{EC-FF}) and forest floor photosynthesis (P_{FF}^{Up}). P_{FF}^{Up} was upscaled from mass-based photosynthesis rates (Eq. 11) and P_C^{EC-FF} was calculated as the difference between the total ecosystem photosynthesis and P_{FF}^{Up} (Eq. 12). The light grey areas illustrate the snow-covered season. For clarity, photosynthesis is represented as a 3-day moving average (For interpretation of the references to colour in this figure legend, the reader is referred to the web version of this article).

Table 3
Yearly cumulative net ecosystem exchange (NEE), total ecosystem respiration (R_E), gross primary production of the whole ecosystem (P_E^{EC}), two estimates for the photosynthesis of the tree canopy, P_C , and two estimates for the forest floor photosynthesis, P_{FF}. Negative NEE indicates that the site was a carbon sink. Values in parentheses are cumulative values from May to September.

	2012	2013	2014	2015
NEE (g C m^{-2} yr^{-1})	−35 (−117)	−48 (−140)	−7 (−77)	14 (−69)
R_E (g C m^{-2} yr^{-1})	492 (333)	553 (373)	529 (375)	489 (321)
P_E^{EC} (g C m^{-2} yr^{-1})	527 (453)	600 (512)	537 (452)	475 (390)
P_C^{EC-Up} (g C m^{-2} yr^{-1})	301 (255)	306 (255)	283 (231)	272 (223)
P_C^{SPP} (g C m^{-2} yr^{-1})	308 (261)	332 (281)	328 (273)	314 (252)
P_{FF}^{Up} (g C m^{-2} yr^{-1})	226 (195)	294 (257)	253 (221)	203 (167)
P_{FF}^{Down} (g C m^{-2} yr^{-1})	219 (188)	269 (231)	208 (179)	161 (138)

Table 4
Slopes and p-values of the linear relationship between different photosynthesis estimates (*P*) for ecosystem (E), canopy (C) and forest floor (FF) together with annual weather characteristics: photosynthetically active radiation (PAR) (μmol m^{-2} s^{-1}), temperature sum (°C) and precipitation (mm). The slope indicates the change in photosynthesis (g C m^{-2} yr^{-1}) per unit of the weather characteristic.

	PAR		Temperature sum		Precipitation	
	Slope	*p*-value	Slope	*p*-value	Slope	*p*-value
P_E^{EC}	1.38	0.04	0.27	0.06	−0.69	0.02
P_C^{EC-Up}	0.36	0.17	0.05	0.39	−0.18	0.16
P_C^{SPP}	0.22	0.33	0.06	0.10	−0.11	0.33
P_{FF}^{Up}	1.01	0.07	0.21	0.01	−0.51	0.05
P_{FF}^{Down}	1.17	0.05	0.21	0.14	−0.58	0.03

meaning that the ecosystem-scale variation was mainly driven by annual variation in forest floor vegetation (Table 4). However, the analysis suffered from a low number of statistically significant relationships even though many *p*-values were relatively low (Table 4).

3.8. Growth variation

The annual length increment of dwarf shrubs showed high variability, and the differences were mainly not significant between years, especially in the evergreen species. However, the growth was lowest in all species in the cold and cloudy summer of 2015, while the differences in growth between years were significant for *V. myrtillus* and *E. nigrum* (Fig. 7). The growth of *V. myrtillus* in 2012 was significantly higher than in other years. The variation in growth was not connected to the variation in the annual P_{FF}^{Down} or P_{FF}^{Up}.

4. Discussion

We studied the CO_2 exchange in a subarctic pine stand in northern Finland for 4 years with distinct weather characteristics and found that during three of these years, the site acted as a weak sink, whereas it was a source of carbon during the coldest and rainiest year with the lowest radiation. The strength of the CO_2 uptake (NEE) was much lower than the mean of forested and tundra sites in Alaska (USA) reported by Ueyama et al. (2013). However, our estimates for GPP in Värriö matched their mean findings. In our study, the total ecosystem respiration was higher than in the Alaskan study and strongly correlated with the temperature sum. The correlation is, on the other hand, evident due to its computational connection to soil temperature (Eq. 3) even though the parameter estimation in one time period (11 days) was independent from other periods. Nevertheless, the relationship between the temperature sum and GPP was even stronger: the carbon sink was largest in the warmest year and lowest in the coldest growing season during the measurement years. This temperature dependency of GPP is in line with several studies (Law et al., 2002; Mäkelä et al., 2008) and our results indicate that without any other modifications, even a relatively small increase in growing season temperature would increase the carbon sink strength of this site. Thus, it seems that the short-term increase in photosynthetic productivity did not increase decomposition unlike that presented by Hartley et al. (2012) and Parker et al. (2015) via the rhizosphere priming effect (Read et al., 2004), but naturally the subject would benefit from a longer time series of high-quality data. The negative correlation between photosynthesis and precipitation most probably just reflected the inverse relationship between radiation and precipitation.

We estimated the photosynthesis of the forest floor using three independent methods: 1) directly measuring carbon fluxes with our subcanopy eddy covariance system, 2) downscaling the flux as a difference between the total ecosystem and estimated canopy photosynthesis (top-down), and 3) upscaling it using the forest floor biomass and available models for leaf-mass based photosynthesis (bottom-up). The overall levels of daily uptake in midsummer were surprisingly similar in all three independent methods (Fig. 4) thus giving credibility to the annual estimates, but each of these methods has significant pros and cons. Potential uncertainties of the three approaches are discussed next.

Firstly, the bottom-up approach considers only the vascular plants and ignores the large biomass of mosses found at our measurement site. Even though their photosynthesis is notably smaller than that of vascular plants (Kulmala, 2011 and references cited therein), they naturally take part in the photosynthetic uptake of the stand (Street et al., 2013). Available leaf-mass based estimates for the maximal photosynthesis of feather mosses range between 4 and 20 nmol g^{-1} s^{-1} (McCall and Martin, 1991; Kulmala et al., 2009, 2011a), whereas those for *V. myrtillus*, *V. vitis-idaea* and *C. vulgaris* are in general five times as high (Kulmala, 2011), varying between 33 and 184 nmol g^{-1} s^{-1} (Widen, 2002; Kolari et al., 2006; Kulmala et al., 2008, 2009, 2011a). In practice, the momentary photosynthesis increased at most by 0.31 or 0.78 g C $m^{-2}day^{-1}$ in 2015 if we assume that 50% of moss biomass is photosynthetically active and leaf-mass based maximal photosynthesis of mosses is 4 or 10 nmol $g^{-1}s^{-1}$, respectively. Annually, this would mean an increase of 19 or 46 g C $m^{-2}yr^{-1}$ i.e. 9% and 22% respectively of the annual GPP of the forest floor vegetation in 2015.

The good fit between the direct measurements and the upscaled photosynthesis accounting only for vascular plants might result from a difference in the leaf-mass based rates adopted from southern and thus more fertile environments compared with this northern study site. A number of studies have found that the rates of photosynthesis per leaf weight, specific leaf area and leaf mass ratio are higher in plants grown in high-nitrogen soils (Field et al., 1983; Field and Mooney, 1983; Poorter et al., 1995; Masarovicova et al., 2000). However, the nitrogen concentrations in Scots pine needles in the site measured by Kulmala et al. (2011a); and the study site do not differ from each other (Palmroth and Hari, 2001; Susiluoto et al., 2010). Besides, Kulmala et al. (2011b) used the PAR at the forest floor, whereas in this study the model uses the PAR measured above the canopy, which might overestimate the photosynthesis of dwarf shrubs and possibly compensate for the impact of missing mosses. Nevertheless, the actual reason behind the good fit between measurements and model remains unknown before revealing the species-specific photosynthesis rates and the radiation environment at the *in-situ* forest floor.

One error source in the upscaling could be the stable leaf biomass used in the calculation. However, most of our species (Table S1) have evergreen leaves with a lifetime of several years, which buffers some effects of the year-to-year variation in the growth of leaf mass. It was also shown by Köster et al. (2017) that the biomass of ground vegetation in northern Finland develops slowly. In addition, the constant leaf mass used in calculating the GPP of the ground vegetation in our study leads to rather close estimates between the direct measurements and the indirect method (Fig. 4), supporting the assumption that the

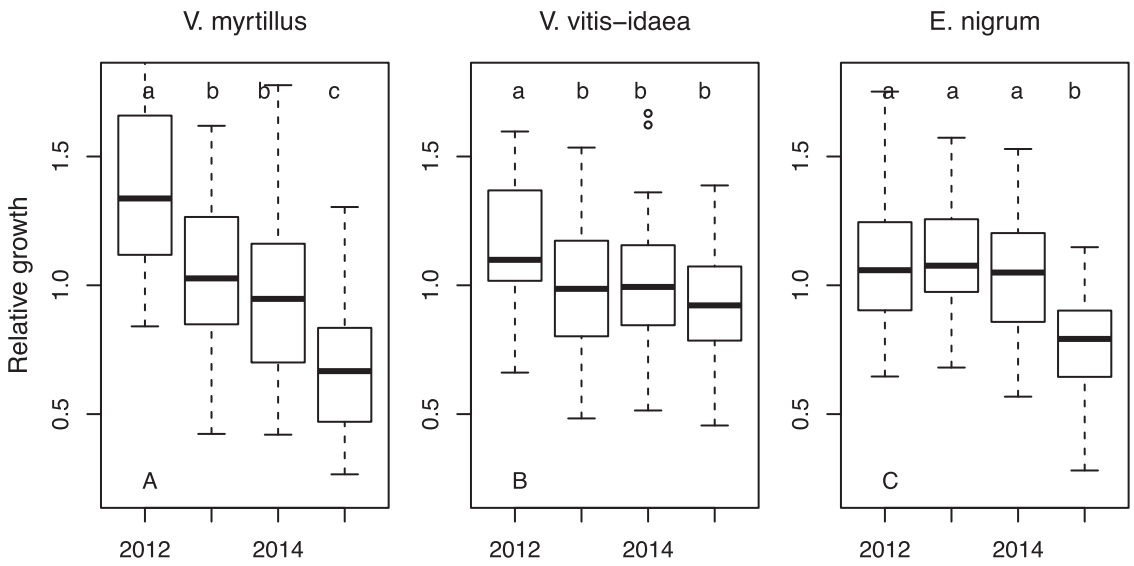

Fig. 7. Relative height increment of *Vaccinium myrtillus* (A), *Vaccinium vitis-idaea* (B) and *Empetrum nigrum* (C) in the different years. The final length differed significantly between years if the lower-case letters differ.

photosynthesizing leaf mass is rather stable. Nevertheless, the use of the introduced photosynthesis model still requires measurements of the overall level of photosynthesis as long as there is no further information available about the biomass variation and the actual leaf-mass based photosynthesis rates at the study area.

Third, the bottom-up model is mainly driven by the temperature and radiation and thus it is evident that the upscaled annual photosynthetic production is higher in sunny and warm growing seasons than in cloudy and cold ones. However, the direct below-canopy eddy covariance measurements and the independent top-down method give a comparable estimate of the daily forest floor photosynthesis, and the latter also of the annual estimate, giving support for the model formulation and result. Thus there is relatively strong evidence that the annual variation in the growing season weather mainly affects the year-to-year variation of forest floor photosynthesis, whereas the tree canopy photosynthesis does not consistently vary with the mean growing season radiation or temperature environment in the observed range.

The importance of canopy structure and especially the light penetration to the ground became evident in our forest floor carbon uptake results. The forest floor vegetation contributed ˜45% to the total ecosystem photosynthetic uptake in this subarctic pine forest. For example, Ikawa et al. (2015) estimated the forest floor vegetation contribution to carbon uptake to be as high as 61% in an open black spruce forest in Alaska. Furthermore, our GPP estimates for the forest floor vegetation (184–266 g C m^{-2}) fall between the estimates in two young Scots pine stands in southern Finland of 349 and 168 g C m^{-2}, with above tree canopy all-sided LAI of 1.4 and 5.1 m^2 m^{-2}, respectively (Kulmala et al., 2009, 2011b). However, most annual estimates of the proportion of forest floor vegetation in the boreal region lie between 10% and 20% (Swanson and Flanagan, 2001; Kolari et al., 2006; Ilvesniemi et al., 2009; Bergeron et al., 2009). Conversely, these estimates are from southern sites with higher canopy coverage than at our subarctic site, suggesting that there might be a clear relationship between the canopy leaf area and the GPP of ground vegetation and thus highlighting motivation for further studies.

There was no clear connection between the variation of GPP and the growth of dwarf shrub shoots, although all species grew less in 2015, which was also the year of low photosynthetic production. Even though it has been shown that the annual variation in the diameter growth of trees is connected to the annual GPP (Berninger et al., 2004; Gea-Izquierdo et al., 2014; Schiestl-Aalto et al., 2015; Kulmala et al., 2016), the buds of most species are usually formed already during the previous year, with the respective late summer temperatures being used to describe the annual variation in the shoot growth of the next growing season (Salminen and Jalkanen, 2005). Nevertheless, the high GPP in 2013 did not seem to affect the height increment in 2014. Probably 4 years of measurements are too short for detecting such growth variation especially when facing lagged responses. Net primary production (NPP), i.e. the growth of biomass, is the difference between photosynthetic production and other carbon sinks such as vital functions, reproduction, changes in internal storage, root exudation, etc. Thus, to obtain a full picture, all other sinks should be subtracted from the primary production. For example, Pumpanen et al. (2012) studied small seedlings and observed that although both photosynthetic production and maintenance respiration increased with increasing temperature, this resulted in an insignificant relationship between temperature and NPP. Also, autocorrelation, changes in leaf area, diseases and other periodical disturbances should be included in order to connect photosynthetic production and growth.

In theory, the fluxes obtained via soil chambers should equal R_{FF}, which was the case in 2015, whereas in 2013–2014, soil chambers showed higher respiration rates than R_{FF} in the middle of the growing season. Thus, our site is among the group of ecosystems in which even R_E is lower than that of soil chamber measurements (Van Gorsel et al., 2007; Wang et al., 2010; Barba et al., 2018). This phenomenon is not fully explained yet, but among the likely causes for this kind of result are footprint related issues, potential error sources in chamber measurement, below-canopy horizontal advection (e.g. Aubinet et al., 2005; Wang et al., 2017), and in the case of ecosystem-scale measurements, also decoupling of below- and above-canopy air mass flow (e.g. Alekseychik et al., 2013; Jocher et al., 2017). The eddy covariance footprints are constantly changing depending on wind and atmospheric stability and thus the two measurement heights integrate fluxes from different areas. Nevertheless, the footprint analysis revealed that not only the location itself but also the extent of the subcanopy footprint (measurement height 2.7 m) overlaps with that of the main tower in the south-western direction. In our study the problem might arise from the chamber measurements as the R_{FF} by those is mostly higher than that of the subcanopy EC measurements. Nevertheless, the estimation of R_E from high latitude eddy covariance data is more complicated compared with that using lower latitude data due to 24 h of daylight and the complexity of defining night-time and hence data partitioning close to midsummer, for example. The daytime method tends to give smaller R_E than the night-time method (Lasslop et al., 2010). However, the

relatively similar estimates for P_{FF} (or P_C) derived with the eddy covariance technique and the independent methods give confidence in the overall level of P_E and thus also in R_E. In addition, our strict filtering policy should remove most of the conditions difficult for eddy covariance measurements, such as calm and stable nights.

5. Conclusions

Northern forests are predicted to experience extensive climate change, which will modify the carbon exchange between ecosystems and the atmosphere. Our results indicate that the studied subarctic site is able to improve its carbon sink if temperature is slightly increased, assuming there are no other climate change related changes. Comparison between canopy and forest floor vegetation revealed that the seasonal dynamics differ especially in springtime when canopy photosynthesis increases approximately one month before snowmelt and the increase of forest floor photosynthesis. This highlights that models of primary production driven without snow cover depth are very likely to inaccurately estimate the seasonal dynamics of photosynthesis in northern forests. That said, the precise modelling of the carbon cycle becomes increasingly important especially regarding the impact of climate change in northern, most rapidly warming ecosystems. We did not find evidence for source limited growth in the annual variation of the height increment of dwarf shrubs, but further studies are required for a better understanding of the sink–source dynamics of growth in these high latitude forests.

Data availability

We have made publicly available the used gap-filled and partitioned eddy covariance data, meteorological records, soil chamber and shoot growth measurements, attained pine shoot chamber parameters and the Stand Photosynthesis Program model input and output as well as the program itself with its graphical user interface. All can be downloaded at: https://b2drop.eudat.eu/s/LzisEZiQG96nDYH

Acknowledgements

We are thankful to Mr Eki Siivola for all technical support and the personnel at Värriö Subarctic Research Station for maintenance of the facilities. The Academy of Finland (grant numbers 277623, 255576, 286190, 286685), the Academy of Finland's Centre of Excellence Programme (grant number 272041) and the Integrated Carbon Observation System Finland (grant number 281255) are acknowledged for financial support.

Appendix A. Supplementary data

Supplementary material related to this article can be found, in the online version, at doi:https://doi.org/10.1016/j.agrformet.2019.02.029.

References

Alekseychik, P., Mammarella, I., Launiainen, S., Rannik, U., Vesala, T., 2013. Evolution of the nocturnal decoupled layer in a Pine forest canopy. Agric. For. Meteorol. 174, 15–27. https://doi.org/10.1016/j.agrformet.2013.01.011.

Aubinet, M., Berbigier, P., Bernhofer, C., Cescatti, A., Feigenwinter, C., Granier, A., Grunwald, T., Havrankova, K., Heinesch, B., Longdoz, B., Marcolla, B., Montagnani, L., Sedlak, P., 2005. Comparing CO2 storage and advection conditions at night at different carboeuroflux sites. Bound -Layer Meteorol. 116, 63–94. https://doi.org/10.1007/s10546-004-7091-8.

Babst, F., Carrer, M., Poulter, B., Urbinati, C., Neuwirth, B., Frank, D., 2012. 500 years of regional forest growth variability and links to climatic extreme events in Europe. Environ. Res. Lett. 7, 045705. https://doi.org/10.1088/1748-9326/7/4/045705.

Baldocchi, D., 1988. A multi-layer model for estimating sulfur-dioxide deposition to a deciduous oak forest canopy. Atmos. Environ. 22, 869–884. https://doi.org/10.1016/0004-6981(88)90264-8.

Barba, J., Cueva, A., Bahn, M., Barron-Gaffordd, G.A., Bond-Lamberty, B., Hanson, P.J., Jaimes, A., Kulmala, L., Pumpanen, J., Scott, R.L., Wohlfahrt, G., Vargas, R., 2018. Comparing ecosystem and soil respiration: review and key challenges of tower-based and soil measurements. Agric. For. Meteorol. 249, 434–443. https://doi.org/10.1016/j.agrformet.2017.10.028.

Bergeron, O., Margolis, H.A., Coursolle, C., 2009. Forest floor carbon exchange of a boreal black spruce forest in eastern North America. Biogeosciences 6, 1849–1864.

Berninger, F., Hari, P., Nikinmaa, E., Lindholm, M., Merilainen, J., 2004. Use of modeled photosynthesis and decomposition to describe tree growth at the northern tree line. Tree Physiol. 24, 193–204.

Burba, G.G., Anderson, D.J., Xu, L., McDermitt, D.K., 2006. Correcting apparent off-season CO2 uptake due to surface heating of an open path gas analyzer: progress report of an ongoing study. Proceedings of 27th Annual Conference of Agricultural and Forest Meteorology 13.

Burba, G.G., McDermitt, D.K., Grelle, A., Anderson, D.J., Xu, L., 2008. Addressing the influence of instrument surface heat exchange on the measurements of CO2 flux from open-path gas analyzers. Global Change Biol. 14, 1854–1876.

Chan, T., Hölttä, T., Berninger, F., Mäkinen, H., Nöjd, P., Mencuccini, M., Nikinmaa, E., 2016. Separating water-potential induced swelling and shrinking from measured radial stem variations reveals a cambial growth and osmotic concentration signal. Plant Cell Environ. 39, 233–244. https://doi.org/10.1111/pce.12541.

Crowther, T.W., Todd-Brown, K.E.O., Rowe, C.W., Wieder, W.R., Carey, J.C., Machmuller, M.B., Snoek, B.L., Fang, S., Zhou, G., Allison, S.D., Blair, J.M., Bridgham, S.D., Burton, A.J., Carrillo, Y., Reich, P.B., Clark, J.S., Classen, A.T., Dijkstra, F.A., Elberling, B., Emmett, B.A., Estiarte, M., Frey, S.D., Guo, J., Harte, J., Jiang, L., Johnson, B.R., Kroel-Dulay, G., Larsen, K.S., Laudon, H., Lavallee, J.M., Luo, Y., Lupascu, M., Ma, L.N., Marhan, S., Michelsen, A., Mohan, J., Niu, S., Pendall, E., Penuelas, J., Pfeifer-Meister, L., Poll, C., Reinsch, S., Reynolds, L.L., Schmidt, I.K., Sistla, S., Sokol, N.W., Templer, P.H., Treseder, K.K., Welker, J.M., Bradford, M.A., 2016. Quantifying global soil carbon losses in response to warming. Nature 540 (104). https://doi.org/10.1038/nature20150.

Davidson, E.A., Janssens, I.A., 2006. Temperature sensitivity of soil carbon decomposition and feedbacks to climate change. Nature 440, 165–173. https://doi.org/10.1038/nature04514.

Fan, S., Gloor, M., Mahlman, J., Pacala, S., Sarmiento, J., Takahashi, T., Tans, P., 1998. A large terrestrial carbon sink in North America implied by atmospheric and oceanic carbon dioxide data and models. Science 282, 442–446. https://doi.org/10.1126/science.282.5388.442.

Field, C., Mooney, H.A., 1983. Leaf age and seasonal effects on light, water, and nitrogen use efficiency in a California shrub. Oecologia 56, 348–355.

Field, C., Merino, J., Mooney, H.A., 1983. Compromises between water-use efficiency and nitrogen-use efficiency in 5 species of California evergreens. Oecologia 60, 384–389.

Foken, T., Wichura, B., 1996. Tools for quality assessment of surface-based flux measurements. Agric. For. Meteorol. 78, 83–105. https://doi.org/10.1016/0168-1923(95)02248-1.

Foken, T., Göckede, M., Mauder, M., Mahrt, L., Amiro, B.D., Munger, J.W., 2004. Post-field data quality control. In: Lee, X., Massman, W.J., Law, B.E. (Eds.), Handbook of Micrometeorology: A Guide for Surface Flux Measurements. Kluwer Academic Publishers, Dordrecht 181-208-181-208.

Gea-Izquierdo, G., Bergeron, Y., Huang, J., Lapointe-Garant, M., Grace, J., Berninger, F., 2014. The relationship between productivity and tree-ring growth in boreal coniferous forests. Boreal Environ. Res. 19, 363–378.

Geissbühler, P., Siegwolf, R., Eugster, W., 2000. Eddy covariance measurements on mountain slopes: the advantage of surface-normal sensor orientation over a vertical set-up. Boundary-Layer Meteorol. 96, 371–392.

Goulden, M.L., Crill, P.M., 1997. Automated measurements of CO2 exchange at the moss surface of a black spruce forest. Tree Physiol. 17, 537–542.

Hari, P., Mäkelä, A., 2003. Annual pattern of photosynthesis in Scots pine in the boreal zone. Tree Physiol. 23, 145–155.

Hari, P., Mäkelä, A., Berninger, F., Pohja, T., 1999. Field evidence for the optimality hypothesis of gas exchange in plants. Aust. J. Plant Physiol. 26, 239–244.

Hartley, I.P., Garnett, M.H., Sommerkorn, M., Hopkins, D.W., Fletcher, B.J., Sloan, V.L., Phoenix, G.K., Wookey, P.A., 2012. A potential loss of carbon associated with greater plant growth in the European Arctic. Nat. Clim. Change 2, 875–879. https://doi.org/10.1038/NCLIMATE1575.

Henttonen, H.M., Mäkinen, H., Heiskanen, J., Peltoniemi, M., Lauren, A., Hordo, M., 2014. Response of radial increment variation of Scots pine to temperature, precipitation and soil water content along a latitudinal gradient across Finland and Estonia. Agric. For. Meteorol. 198, 294–308. https://doi.org/10.1016/j.agrformet.2014.09.004.

Ikawa, H., Nakai, T., Busey, R.C., Kim, Y., Kobayashi, H., Nagai, S., Ueyama, M., Saito, K., Nagano, H., Suzuki, R., Hinzman, L., 2015. Understory CO2, sensible heat, and latent heat fluxes in a black spruce forest in interior Alaska. Agric. For. Meteorol. 214, 80–90. https://doi.org/10.1016/j.agrformet.2015.08.247.

Ilvesniemi, H., Levula, J., Ojansuu, R., Kolari, P., Kulmala, L., Pumpanen, J., Launiainen, S., Vesala, T., Nikinmaa, E., 2009. Long-term measurements of the carbon balance of a boreal Scots pine dominated forest ecosystem. Boreal Environ. Res. 14, 731–753.

Jocher, G., Lofvenius, M.O., De Simon, G., Hornlund, T., Linder, S., Lundmark, T., Marshall, J., Nilsson, M.B., Nasholm, T., Tarvainen, L., Oquist, M., Peichl, M., 2017. Apparent winter CO2 uptake by a boreal forest due to decoupling. Agric. For. Meteorol. 232, 23–34. https://doi.org/10.1016/j.agrformet.2016.08.002.

Kaimai, J., Gaynor, J., 1991. Another look at sonic thermometry. Boundary-Layer Meteorol. 56, 401–410. https://doi.org/10.1007/BF00119215.

Kljun, N., Calanca, P., Rotach, M.W., Schmid, H.P., 2005. A simple parameterisation for flux footprint predictions. Boundary-Layer Meteorol. 112, 503–523.

Kolari, P., Pumpanen, J., Kulmala, L., Ilvesniemi, H., Nikinmaa, E., Gronholm, T., Hari, P., 2006. Forest floor vegetation plays an important role in photosynthetic production of boreal forests. For. Ecol. Manage. 221, 241–248. https://doi.org/10.1016/j.foreco.2005.10.021.

Kolari, P., Lappalainen, H.K., Hänninen, H., Hari, P., 2007. Relationship between temperature and the seasonal course of photosynthesis in Scots pine at northern timberline and in southern boreal zone. Tellus B Chem. Phys. Meteorol. 59, 542–552.

https://doi.org/10.1111/j.1600-0889.2007.00262.x.
Kolari, P., Chan, T., Porcar-Castell, A., Bäck, J., Nikinmaa, E., Juurola, E., 2014. Field and controlled environment measurements show strong seasonal acclimation in photosynthesis and respiration potential in boreal Scots pine. Front. Plant Sci. 5, 717. https://doi.org/10.3389/fpls.2014.00717.
Kormann, R., Meixner, F.X., 2001. An analytical footprint model for non-neutral stratification. Boundary-Layer Meteorol. 99 (2), 207–224.
Körner, C., 2003. Carbon limitation in trees. J. Ecol. 91, 4–17. https://doi.org/10.1046/j.1365-2745.2003.00742.x.
Korpela, M., Nöjd, P., Hollmen, J., Mäkinen, H., Sulkava, M., Hari, P., 2011. Photosynthesis, temperature and radial growth of Scots pine in northern Finland: identifying the influential time intervals. Trees-Struct. Funct. 25, 323–332. https://doi.org/10.1007/s00468-010-0508-8.
Köster, K., Köster, E., Kulmala, L., Berninger, F., Pumpanen, J., 2017. Are the climatic factors combined with reindeer grazing affecting the soil CO2 emissions in subarctic boreal pine forest? Catena 149 (616). https://doi.org/10.1016/j.catena.2016.06.011.
Kulmala, L., 2011. Photosynthesis of Ground Vegetation in Boreal Scots Pine Forests. 45 p. Available from:. University of Helsinki, Helsinki, Finland. https://helda.helsinki.fi/handle/10138/27969.
Kulmala, L., Launiainen, S., Pumpanen, J., Lankreijer, H., Lindroth, A., Hari, P., Vesala, T., 2008. H2O and CO2 fluxes at the floor of a boreal pine forest. Tellus Series B-Chem. Phys. Meteorol. 60, 167–178. https://doi.org/10.1111/j.1600-0889.2007.00327.x.
Kulmala, L., Pumpanen, J., Vesala, T., Hari, P., 2009. Photosynthesis of boreal ground vegetation after a forest clear-cut. Biogeosciences 6, 2495–2507.
Kulmala, L., Pumpanen, J., Hari, P., Vesala, T., 2011a. Photosynthesis of ground vegetation in different aged pine forests: effect of environmental factors predicted with a process-based model. J. Veg. Sci. 22, 96–111.
Kulmala, L., Pumpanen, J., Kolari, P., Muukkonen, P., Hari, P., Vesala, T., 2011b. Photosynthetic production of ground vegetation in different-aged Scots pine (Pinus sylvestris) forests. Can. J. For. Res. 41, 2020–2030. https://doi.org/10.1139/X11-121.
Kulmala, L., Žliobaitė, I., Nikinmaa, E., Nöjd, P., Kolari, P., Koupaei, K.K., Hollmén, J., Mäkinen, H., 2016. Environmental control of growth variation in a boreal Scots pine stand - a data-driven approach. Silva Fenn. 50. https://doi.org/10.14214/sf.1680.
Kulmala, L., Read, J., Nöjd, P., Rathgeber, C.B.K., Cuny, H.E., Hollmén, J., Mäkinen, H., 2017. The main drivers for the division and maturation of Scots pine tracheids along a temperature gradient. Agric. For. Meteorol. 232, 210–224.
Lasslop, G., Reichstein, M., Papale, D., Richardson, A.D., Arneth, A., Barr, A., Stoy, P., Wohlfahrt, G., 2010. Separation of net ecosystem exchange into assimilation and respiration using a light response curve approach: critical issues and global evaluation. Global Change Biol. 16, 187–208. https://doi.org/10.1111/j.1365-2486.2009.02041.x.
Launiainen, S., Rinne, J., Pumpanen, J., Kulmala, L., Kolari, P., Keronen, P., Siivola, E., Pohja, T., Hari, P., Vesala, T., 2005. Eddy covariance measurements of CO2 and sensible and latent heat fluxes during a full year in a boreal pine forest trunk-space. Boreal Environ. Res. 10, 569–588.
Law, B., Falge, E., Gu, L., Baldocchi, D., Bakwin, P., Berbigier, P., Davis, K., Dolman, A., Falk, M., Fuentes, J., Goldstein, A., Granier, A., Grelle, A., Hollinger, D., Janssens, I., Jarvis, P., Jensen, N., Katul, G., Mahli, Y., Matteucci, G., Meyers, T., Monson, R., Munger, W., Oechel, W., Olson, R., Pilegaard, K., Paw, K., Thorgeirsson, H., Valentini, R., Verma, S., Vesala, T., Wilson, K., Wofsy, S., 2002. Environmental controls over carbon dioxide and water vapor exchange of terrestrial vegetation. Agric. For. Meteorol. 113, 97–120. https://doi.org/10.1016/S0168-1923(02)00104-1.
Mäkelä, A., Hari, P., Berninger, F., Hänninen, H., Nikinmaa, E., 2004. Acclimation of photosynthetic capacity in Scots pine to the annual cycle of temperature. Tree Physiol. 24, 369–376.
Mäkelä, A., Kolari, P., Karimaki, J., Nikinmaa, E., Perämäki, M., Hari, P., 2006. Modelling five years of weather-driven variation of GPP in a boreal forest. Agric. For. Meteorol. 139, 382–398. https://doi.org/10.1016/j.agrformet.2006.08.017.
Mäkelä, A., Pulkkinen, M., Kolari, P., Lagergren, F., Berbigier, P., Lindroth, A., Loustau, D., Nikinmaa, E., Vesala, T., Hari, P., 2008. Developing an empirical model of stand GPP with the LUE approach: analysis of eddy covariance data at five contrasting conifer sites in Europe. Global Change Biol. 14, 92–108. https://doi.org/10.1111/j.1365-2486.2007.01463.x.
Masarovicova, E., Welschen, R., Lux, A., Mikus, M., Lambers, H., 2000. The response of the perennial teosinte Zea diploperennis (Poaceae) to nitrate availability. Maydica 45, 13–19.
Massman, W., 2000. A simple method for estimating frequency response corrections for eddy covariance systems. Agric. For. Meteorol. 104, 185–198. https://doi.org/10.1016/S0168-1923(00)00164-7.
McCall, K.K., Martin, C.E., 1991. Chlorophyll concentrations and photosynthesis in three forest understory mosses in Northeastern Kansas. Bryologist 94, 25–29.
Moren, A.S., Lindroth, A., 2000. CO2 exchange at the floor of a boreal forest. Agric. For. Meteorol. 101, 1–14.
Myneni, R., Keeling, C., Tucker, C., Asrar, G., Nemani, R., 1997. Increased plant growth in the northern high latitudes from 1981 to 1991. Nature 386, 698–702. https://doi.org/10.1038/386698a0.
Palmroth, S., Hari, P., 2001. Evaluation of the importance of acclimation of needle structure, photosynthesis, and respiration to available photosynthetically active radiation in a Scots pine canopy. Can. J. Res. 31, 1235–1243 https://doi-org.libproxy.helsinki.fi/10.1139/x01-051.
Parker, T.C., Subke, J., Wookey, P.A., 2015. Rapid carbon turnover beneath shrub and tree vegetation is associated with low soil carbon stocks at a subarctic treeline. Global Change Biol. 21, 2070–2081. https://doi.org/10.1111/gcb.12793.
Pelkonen, P., Hari, P., 1980. The dependence of the springtime recovery of Co2 uptake in scots pine on temperature and internal factors. Flora 169, 398–404.
Pirinen, P., Simola, H., Aalto, J., Kaukoranta, J.-, Karlsson, P., Ruuhela, R. (Eds.), 2012. Tilastoja Suomen Ilmastosta 1981-2010 - Climatological Statistics of Finland Climatological Statistics of Finland 1981–2010. Finnish Meteorological Institute, Helsinki, Finland 83 p.
Poorter, H., Vijver, C., van de B, R.G., Lambers, H., 1995. Growth and carbon economy of a fast-growing and a slow-growing grass species as dependent on nitrate supply. Plant Soil 171, 217–227.
Pumpanen, J., Heinonsalo, J., Rasilo, T., Villemot, J., Ilvesniemi, H., 2012. The effects of soil and air temperature on CO2 exchange and net biomass accumulation in Norway spruce, Scots pine and silver birch seedlings. Tree Physiol. 32, 724–736. https://doi.org/10.1093/treephys/tps007.
Pumpanen, J., Kulmala, L., Linden, A., Kolari, P., Nikinmaa, E., Hari, P., 2015. Seasonal dynamics of autotrophic respiration in boreal forest soil estimated by continuous chamber measurements. Boreal Environ. Res. 20, 637–650.
Qian, H., Joseph, R., Zeng, N., 2010. Enhanced terrestrial carbon uptake in the northern high latitudes in the 21st century from the coupled carbon cycle climate model intercomparison project model projections. Global Change Biol. 16, 641–656. https://doi.org/10.1111/j.1365-2486.2009.01989.x.
Read, D., Leake, J., Perez-Moreno, J., 2004. Mycorrhizal fungi as drivers of ecosystem processes in heathland and boreal forest biomes. Can. J. Bot. –Rev. Can. Bot. 82, 1243–1263. https://doi.org/10.1139/B04-123.
Repola, J., 2009. Biomass equations for scots pine and Norway spruce in Finland. Silva Fenn 43, 625–647. https://doi.org/10.14214/sf.184.
Salminen, H., Jalkanen, R., 2005. Modelling the effect of temperature on height increment of Scots pine at high latitudes. Silva Fenn 39, 497–508. https://doi.org/10.14214/sf.362.
Schiestl-Aalto, P., Kulmala, L., Mäkinen, H., Nikinmaa, E., Mäkelä, A., 2015. CASSIA - a dynamic model for predicting intra-annual sink demand and interannual growth variation in Scots pine. New Phytol. 206, 647–659. https://doi.org/10.1111/nph.13275.
Schotanus, P., Nieuwstadt, F., Debruin, H., 1983. Temperature-measurement with a sonic anemometer and its application to heat and moisture fluxes. Bound -Layer Meteorol. 26, 81–93. https://doi.org/10.1007/BF00164332.
Seo, J., Eckstein, D., Jalkanen, R., Schmitt, U., 2011. Climatic control of intra- and interannual wood-formation dynamics of Scots pine in northern Finland. Environ. Exp. Bot. 72, 422–431. https://doi.org/10.1016/j.envexpbot.2011.01.003.
Speckman, H.N., Frank, J.M., Bradford, J.B., Miles, B.L., Massman, W.J., Parton, W.J., Ryan, M.G., 2015. Forest ecosystem respiration estimated from eddy covariance and chamber measurements under high turbulence and substantial tree mortality from bark beetles. Global Change Biol. 21, 708–721. https://doi.org/10.1111/gcb.12731.
Street, L.E., Subke, J., Sommerkorn, M., Sloan, V., Ducrotoy, H., Phoenix, G.K., Williams, M., 2013. The role of mosses in carbon uptake and partitioning in arctic vegetation. New Phytol. 199, 163–175. https://doi.org/10.1111/nph.12285.
Subke, J.A., Tenhunen, J.D., 2004. Direct measurements of CO2 flux below a spruce forest canopy. Agric. For. Meteorol. 126, 157–168. https://doi.org/10.1016/j.agrformet.2004.06.007 ER.
Susiluoto, S., Hilasvuori, E., Berninger, F., 2010. Testing the growth limitation hypothesis for subarctic Scots pine. J. Ecol. 98, 1186–1195. https://doi.org/10.1111/j.1365-2745.2010.01684.x.
Swanson, R.V., Flanagan, L.B., 2001. Environmental regulation of carbon dioxide exchange at the forest floor in a boreal black spruce ecosystem. Agric. For. Meteorol. 108, 165–181.
Ueyama, M., Iwata, H., Harazono, Y., Euskirchen, E.S., Oechel, W.C., Zona, D., 2013. Growing season and spatial variations of carbon fluxes of Arctic and boreal ecosystems in Alaska (USA). Ecol. Appl. 23, 1798–1816. https://doi.org/10.1890/11-0875.1.
Ueyama, M., Kudo, S., Iwama, C., Nagano, H., Kobayashi, H., Harazono, Y., Yoshikawa, K., 2015. Does summer warming reduce black spruce productivity in interior Alaska? J. For. Res. 20, 52–59. https://doi.org/10.1007/s10310-014-0448-z.
Van Gorsel, E., Leuning, R., Cleugh, H.A., Keith, H., Suni, T., 2007. Nocturnal carbon efflux: reconciliation of eddy covariance and chamber measurements using an alternative to the u(*)-threshold filtering technique. Tellus Series B-Chem. Phys. Meteorol. 59, 397–403. https://doi.org/10.1111/j.1600-0889.2007.00252.x.
Vesala, T., Launiainen, S., Kolari, P., Pumpanen, J., Sevanto, S., Hari, P., Nikinmaa, E., Kaski, P., Mannila, H., Ukkonen, E., Piao, S.L., Ciais, P., 2010. Autumn temperature and carbon balance of a boreal Scots pine forest in Southern Finland. Biogeosciences 7, 163–176. https://doi.org/10.5194/bg-7-163-2010.
Vickers, D., Mahrt, L., 1997. Quality control and flux sampling problems for tower and aircraft data. J. Atmos. Ocean Technol. 14, 512–526. https://doi.org/10.1175/1520-0426(1997)0142.0.CO;2.
Wang, M., Guan, D., Han, S., Wu, J., 2010. Comparison of eddy covariance and chamber-based methods for measuring CO2 flux in a temperate mixed forest. Tree Physiol. 30, 149–163. https://doi.org/10.1093/treephys/tpp098.
Wang, X., Wang, C., Bond-Lamberty, B., 2017. Quantifying and reducing the differences in forest CO2-fluxes estimated by eddy covariance, biometric and chamber methods: a global synthesis. Agric. For. Meteorol. 247, 93–103. https://doi.org/10.1016/j.agrformet.2017.07.023.
Webb, E.K., Pearman, G.I., Leuning, R., 1980. Correction of flux measurements for density effects due to heat and water vapour transfer. Q. J. R. Meteorol. Soc. 106, 85–100.
Widen, B., 2002. Seasonal variation in forest-floor CO2 exchange in a Swedish coniferous forest. Agric. For. Meteorol. 111, 283–297.
Xu, B., Yang, Y., Li, P., Shen, H., Fang, J., 2014. Global patterns of ecosystem carbon flux in forests: a biometric data-based synthesis. Global Biogeochem. Cycles 28, 962–973. https://doi.org/10.1002/2013GB004593.